Energy Losses during Intestine Deformation – A New Method of Robot Propulsion?

Łukasz Frączczak, Paweł Żak, Michał Starosta

Institute of Machine Tools and Production Engineering, Lodz University of Technology, Stefanowskiego 1/15, 90-924 Lodz, Poland;
lukasz.fracczak@p.lodz.pl, pawel.zak@p.lodz.pl, michal.starosta@dokt.p.lodz.pl

Abstract: Currently, numerous studies are conducted on diagnostic devices for the digestive system. To correctly design such a device, it is necessary to fully specify the parameters of the environment in which the device is supposed to operate. Most of the research conducted on the intestines focuses on mechanical and tribological parameters connected to work with diagnostic capsules. Yet, to simulate the work of the robot moving with a snake-like motion it is necessary to estimate the level of energy dissipated by the intestine deformation as it serves as a main driving factor, which is proven in the paper.

Keywords: intestine mechanical parameters; energy dissipation; robot propulsion

1 Introduction

The development in the field of mobile robotics is determined by the knowledge of the work environment. The same goes for robots prepared to move inside the human body. One good example of such a case is in the field of robotics focused on the diagnosis and treatment of the human digestive system. This field is extremely important, as it aids doctors in the treatment of digestive system disease, including intestinal cancer, therefore, many studies are being conducted on developing the most universal tool. The most commonly used method is the capsule endoscopy [1], which utilises a small-volume capsule that travels through the digestive system, taking photos or picking tissue samples in the process. Yet, there is hardly any control over such capsule motion. An interesting example of a different solution is a robot able to move inside the intestines using a snake-like motion [2]. In Figure 1 an actual model of a named robot is presented. The given picture shows the robot’s motion capabilities. It is worth mentioning that because of its construction, it is able to generate sine motion, which is necessary to make its motion possible in any given position or configuration of the body. The dimensions of the presented model currently are: 15 mm of diameter and ca. 1.5 m of length. The remaining question is: will it be able to move inside the human body according to the assumptions?

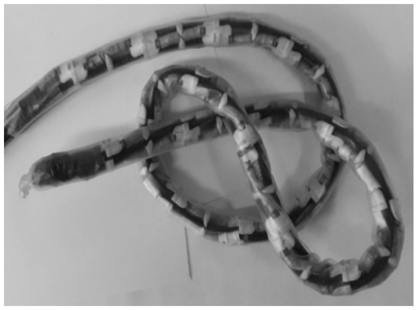

Figure 1
Actual model of the robot moving with snake-like motion

This type of motion is difficult in this environment, as it acts like a visco-elastic body [3]. Assume that a robot moving using a snake-like motion (close to sine) would deform the intestines in a direction perpendicular to its own body (Fig. 2).

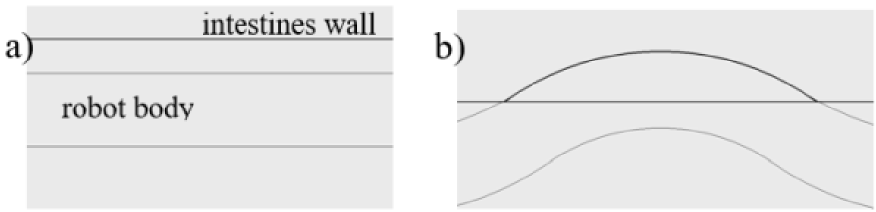

Figure 2
Deformation of the intestine by the robot: a) before deformation, b) after deformation

In this case, a 2D static model of the robot–intestine system shows reaction forces between the robot and the intestines, without internal forces analysis, will take the form shown in Fig. 3. The additional assumption made was that the robot's deformation will take a shape close to a circle.

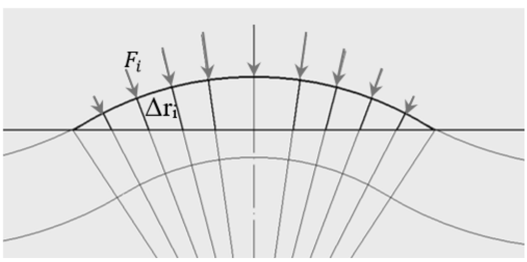

Figure 3
Reaction forces between the robot and the intestines

For this assumption, the work needed to be done to deform the intestines can be given by the following equation:

$$W = E_p + \Delta E \quad (1)$$

Where W – work done to deform the intestines, E_p – potential energy accumulated in the deformed intestines, ΔE – energy that was dissipated in the intestines and cannot be reclaimed.

With the assumption that the intestines are being deformed perpendicularly to the robot's surface, the deformation energy of the intestines can be given as:

$$E_p = \frac{1}{2}\sum_{i=1}^{n} F_i * \Delta r_i \quad (2)$$

Where: F_i is the force with which the robot deformed the intestines in the i-th contact point, Δr_i – the intestine deformation in a direction normal to the robot's surface.

Equation (2) is true for symmetrical deformation, i.e., for the robot moving perpendicularly to the intestinal wall. In the case of the robot generating a propulsion wave along its body, the part of the intestines in front of the wave is being deformed while the part located after the deformation wave reacts to the robot with the force generated by its elasticity. In this case, the geometry of the system can be presented as in Fig. 4.

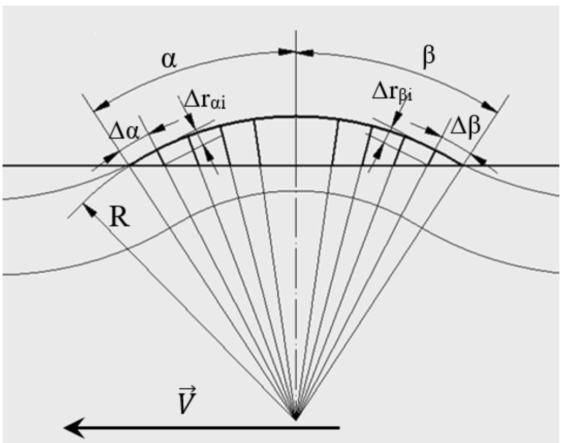

Figure 4

The distribution of deformation geometry for the robot moving with a snake-like motion

The equations of deformation energy can be defined as:

$$W_L = \frac{1}{2}\sum_{i=1}^{n} F_{\alpha i} * \Delta r_{\alpha i} + \Delta E_L \quad (3)$$

$$W_R = \frac{1}{2}\sum_{i=1}^{n} F_{\beta j} * \Delta r_{\beta j} + \Delta E_R \tag{4}$$

Where: W_L, is the work that need to be done to deform the intestines, W_R is the work done by the intestines regaining their original shape, $F_{\alpha i}$ – is the i-th force acting on the left side of the robot, $F_{\beta i}$ – is the j-th force acting on the right side of the robot, $\Delta r_{\alpha i}$, $\Delta r_{\beta j}$ – are the i-th and j-th deformation of the intestines done by the robot at the left and right side. $\Delta E_L = f(\alpha, D, T, t)$ and $\Delta E_R = f(\beta, D, T, t)$ are the energies dissipated during the deformation during the elongation and shape regaining phases of the intestines.

In case of respectively small increases of $\Delta r_{\alpha i}$ and $\Delta r_{\beta j}$ equations (3, 4) take the following form:

$$W_L = \frac{1}{2}\int_0^{\alpha} F(\alpha) * r(\alpha) d\alpha + \Delta E_L \tag{5}$$

$$W_R = \frac{1}{2}\int_0^{\beta} F(\beta) * r(\beta) d\beta + \Delta E_R \tag{6}$$

For symmetrical deformations (case of the robot moving perpendicularly to intestines wall) and for perfectly elastic deformations (ΔE_L=0 and ΔE_R=0), it can be stated that $W_L = W_R$. Yet, in the case when the robot moves with a snake-like motion, the work done by the intestines regaining their shape is equal to the potential energy accumulated in the intestines and can be given with equation:

$$E_p = W_L - \Delta E_L = W_R \tag{7}$$

By including equations (5), (6) in (7) the following is obtained:

$$\frac{1}{2}\int_0^{\alpha} F(\alpha) * r(\alpha) d\alpha = \frac{1}{2}\int_0^{\beta} F(\beta) * r(\beta) d\beta + \Delta E_R \tag{8}$$

It must be stated that the total deformations on the left and right sides of equation (8) must be equal. Otherwise, the intestines would remain permanently deformed, which is unacceptable. Therefore, the following equation is true:

$$\int_0^{\alpha} r(\alpha) d\alpha = \int_0^{\beta} r(\beta) d\beta \tag{9}$$

By comparing equations (8) and (9), it can be seen that energy loss is bound with the reaction forces that caused the deformation. By assuming that the system shown in Fig. 2 is static and by projecting all the forces onto the direction of the wave, the following is obtained:

$$F_L = \sum_{i=1}^{n} F_{\alpha i} * cos\alpha_i \quad (10)$$

$$F_R = \sum_{i=1}^{n} F_{\beta j} * cos\beta_j \quad (11)$$

and from (7) and (8) it is known that $F_L > F_R$

It can be stated that:

$$F_c - T = F_L - F_R \quad (12)$$

Where: F_c is the total force of intestinal reaction on the robot in the direction of wave propagation, T – is the friction force, F_L, F_R are the forces respectively before and after the deformation wave.

Equations (12) and (8) show that the forces needed to be used to deform the intestines are greater than forces generated by the intestines regaining their original shape, therefore by generating the snake-like motion force Fc is generated. It is directed along with the robot and reverses to the direction of the wave of displacements. Equation (8) clearly shows that propulsion forces will increase proportionally to the volume of Energy dissipated during intestine deformation. It shows the necessity of checking how much of the energy is dissipated during intestine deformation. The proposed research will provide data necessary to estimate the volume of force possible to be generated by a robot moving with a snake-like motion.

Increasing understanding of the mechanical characteristics of the intestines took on particular importance in the context of the development of new medical instruments (e.g., capsule robot, intellectualized endoscopy). A significant element of this understanding is gaining information about the mechanical influence between the intestinal tissue and the instrument.

To obtain information about the stresses and strains (and their relations) which accompany the biomechanical changes during functional loading and unloading of the human gastrointestinal (GI) tract, a reference was made to Hans Gregersen's research [4]. As a basis for 3D anatomical models, digital images gained through ultrasound, using computer tomography (CT) or magnetic resonance (MRI) were used. Models were analyzed using different mathematical algorithms - the finite elements method (in this particular example of the mucosal folded three-layered esophagus) and assuming that it is a thin-walled isotropic structure (e.g. stomach antrum wall surface model). The finite element method provides the possibility to overcome the major shortcoming connected with the thin wall assumption.

The research, focused on gaining information about the mechanical characteristics of the intestines, included two aspects of influence between the medical instrument and the intestinal tissue: the "frictional force" and the biomechanics of GI tract tissue.

The rest of the paper is organised as follows: Sections 2 and 3 focus on state-of-the-art clarification, while Sections 4-6 describe tests done on actual tissues including a description of a tests stand, used methods and drawn conclusions.

2 Frictional Force

The frictional resistance force includes the nominal frictional force [5] and the visco-adhesive force and it depends on the size, material, mass, shape, contact surface contour, and the velocity of the potential instrument (e.g. capsule robot) [6] [7]. The nominal frictional force is related to the elastic restoring force, the real frictional force, and the contact angle; the cohesive force is determined by the contact area and the contact angle [7]. Ex-vivo experiments were carried out in the porcine small intestine with fifteen capsule robots (capsule endoscope) with different shapes and dimensions [8]. The friction increased accordingly with the speed and capsule dimensions, especially by the dimensions perpendicular to the moving direction. To predict the behavior of the capsule robot in clinical tests, the analytical friction model of the capsule robot in the small intestine has been researched [9]. In addition, the results of a similar experimental investigation proved that the Coefficient of Friction (COF) did not change significantly concerning the apparent area of contact between the capsule and the intestine. The COF decreased with an increase in the normal load and varied from 0.08 to 0.2 [10]. In the case of capsule robots with their locomotive mechanism, the stroke of the capsule also influences the friction force [11]. During consideration of the self-propelled robotic endoscope concept, it is extremely important to keep in mind that locomotion in the small intestine is further complicated by the fact that the intestine is not a rigid pipe and is susceptible to damage [12]. The presented analysis states that the friction coefficient between the intestines and the endoscope capsule or robot takes an important role in moving the device inside the intestine, but the research has been conducted only on the motion of the endoscope capsule. In the case of the drive of a device moving with snake-like motion, the key will be the mechanical parameters of the intestines in addition to friction forces.

3 Intestines Mechanical Examination

An example of mechanical tests of research on the viscoelasticity of intestines was obtained by the use of a Dynamical Mechanical Analyzer (DMA) [4]. In this work, it was proven that the dynamic mechanical parameters of the intestinal tissues are not always steady, especially when forced oscillation happens. In practice, this means that the movement of the medical instrument would work in a changing environment, and during the modeling of the intestine, the variation should be taken into account. Based on the sheer measurement of the DMA and the stress relaxation measurement, a five-element model describing the viscoelasticity of intestines was obtained. Additionally, the DMA tests indicate that the storage modulus descends with the increasing shear strain, which means the hyper-elasticity of the small intestine can be measured numerically. As a consequence, the obtained data could be the basis for numerical calculations and the relaxation modulus could be also calculated [13].

Similar experimental investigations of stress relaxation and the stress-strain relations have also proven that the small intestine shows the typical behavior of a viscoelastic material [14]. Dynamic testing results show that the storage modulus of the intestine decreases first and then increases when the frequency is raised within the range of 1-20 Hz [14].

Results of an experimental study of the in vivo and ex vivo compression of goat large intestine revealed a significant difference between the results at the lower and higher rates in in-vivo tests (at the lower rates, the tissue appeared softer) [6]. What is also important, there was a difference between the results of the in vivo and in vitro tests. In vitro results showed less dependence on the compression rates, when the in vivo results were strongly dependent on the compression rates. There is a risk of using only in vitro data in numerical simulations of modeling tissue [6]. An analogous experimental study of the in vitro compression of dog intestine presents very comparable results. The shape and parameters of the curves obtained were very close to the analysis of goat tissues. The incremental elastic modulus of the duodenum of the dog was larger than that of the jejunum under particular pressure [15].

The tensile properties of the human GI tract tissues (including the small and large intestine) generated for cadaveric and surgically removed specimens have been also examined in several experimental investigations. The values of maximal stress and destructive strain were the following: for small intestine transversal specimens - 0.9 MPa and 140% and for large intestine transversal specimens - 0.9 MPa and 180%. [16] The submucosa and muscular layers condition the mechanical strength of the intestine wall; serosa and mucosa showed no significant strength.

As shown, tests on the intestines' mechanical parameters are nothing new. Most of the research has been conducted focusing on selected device types, mainly a

Capsule Robot (CR). Yet, to date, no research had been done to test the intestines with a snake-like motion. It will be crucial to test viscoelasticity [4] and damping [13] factors, friction forces and to estimate the energy dissipated in the intestines. The parameters mentioned at the end are definitive for the use of the phenomena that while deforming the intestines the force applied to deform them is greater than the force generated by intestines returning to their original shape. The difference in forces can be used to propel the device moving inside the digestive tract. The interaction between selected parts of the intestines will be important along with the energy dissipated during the intestine elongation. Another important task connected to the determination of the intestines' mechanical parameters is the possibility to implement them into simulation software. The more accurate the parameters are, the more accurate the obtained simulation results will be.

4 Materials and Methods

Tests on the dynamic parameters of the intestines were made using the custom-made test stand presented in Figure 5. It consists of a linear drive with a positioning accuracy of 0.01 mm and regulated feed in the range from 0 to 100 mm/s. On the carrier of the drive, a 6-axis force sensor has been placed along with a diagnostic probe.

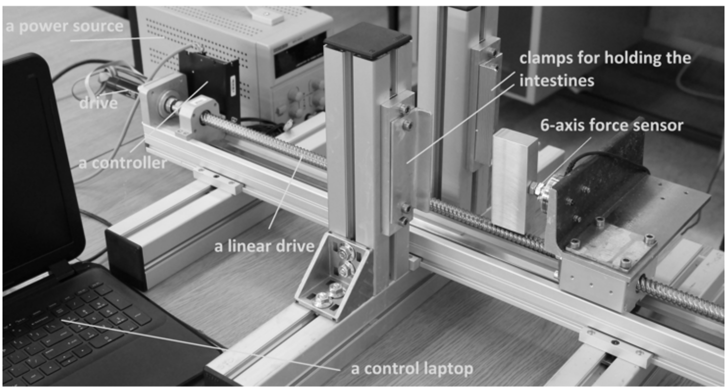

Figure 5
A test stand

The stand has been used to perform numerous tests the purpose of which was to estimate the intestines' elasticity curve and to estimate the volume of the energy dissipated during their deformation. The intestines were taken from pigs just after being slaughtered. During transport, they were kept at a temperature of 3^{o} C, next they were initially cleaned and placed in saline. Before the experiment, the samples were heated to the ambient temperature of ca. 23° C. The time between taking the sample and the test ranged from 40 minutes for the first sample up to 90 minutes for the last one. The tests were made with forces not causing damage to the samples. During the preliminary test phase, ten repeats were done to specify minimal breaking force, which was estimated at ca. 20 N. Therefore, the tests were made keeping the forces under 15 N.

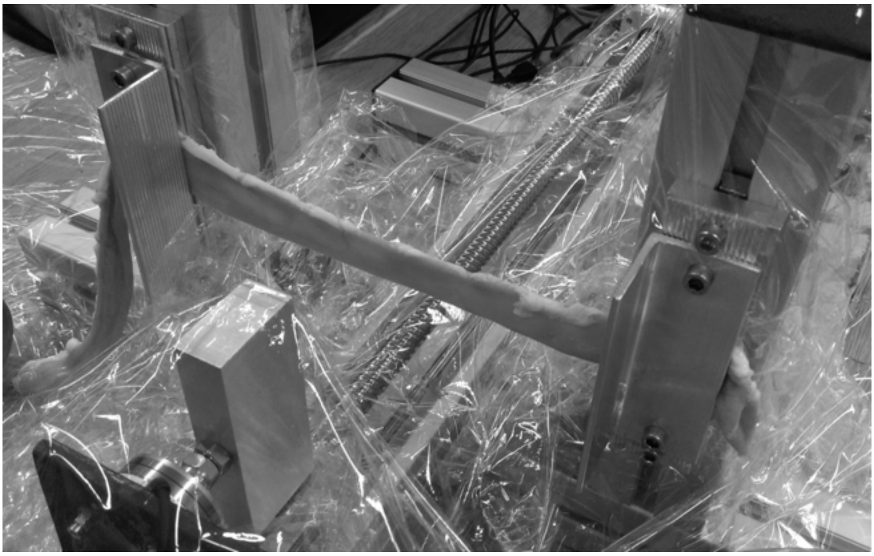

Figure 6
A fixed intestines sample

The sample was placed in holders (the distance between them was 87.3 mm) on the stand presented in Figure 6. The intestines were initially stretched with a force of ca. 3 N magnitude. Next, the diagnostic probe was moved toward the intestines while keeping the force sensor level of 0 N. After that, the test probe was moved in a direction perpendicular to the intestinal axis stretching them, and then it was moved back to the initial position. The displacements and forces generated were recalculated into displacements in a longitudinal direction. Such displacements were made five times for five simples with three different elongations each time. The results of the sample tests can be seen in Figure 7. It shows that the forces of stretching the intestines (right direction) are greater than the forces of the intestine acting on the sensor during the release motion (left direction). The volume of force dissipated in this system is the difference of the surface areas under the diagram of stretching and releasing, therefore it can be expressed with the following equation:

$$\Delta E = \int_{l_0}^{l} f(l)dl - \int_{l_0}^{l} f'(l)dl = \int_{l_0}^{l} \left(f(l) - f'(l)\right)dl \tag{13}$$

where: f(l), f'(l) are the stretching and release force curves, l – the maximum length of the intestine in maximum elongation for which motion direction change occurred, l_0 - preliminary elongation of the sample.

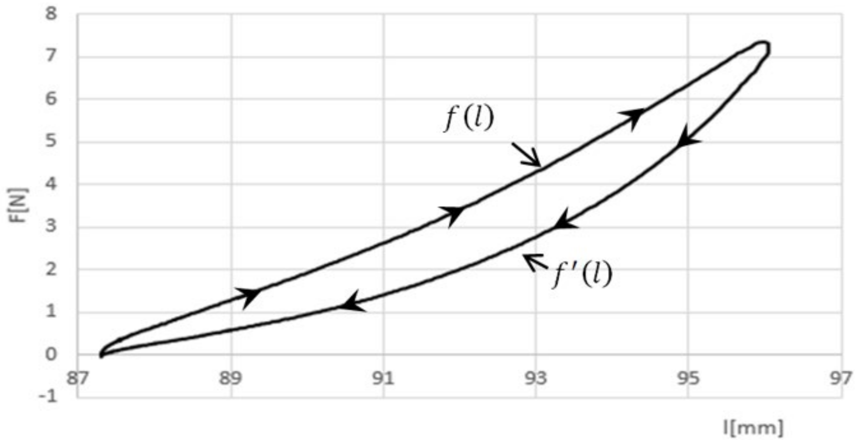

Figure 7
Force curve for longitudal elongation of the intestines by 9 mm (10%) and return to the preliminary position

5 Results

To check how much energy is dissipated in intestines deformations. There were 18 intestines samples tested. The samples were elongated with different values: 7; 10; 13% of their length. Three other samples were tested with different elongation with changing elongation speed from 3.3 to 83.3 mm/s.

The calculation results are summarized in Tables 1 and 2. Table 1 shows the results of five samples and five elongations of the intestines and Table 2 shows the average values of five elongations for each of the five samples. In addition, three different test series with variating elongation values are shown in this table.

Table 1
Value of dissipated energy and maximum forces in intestines elongation by 9mm (10%)

			Stretching					
			1	**2**	**3**	**4**	**5**	**Average**
Sample 1	**Max force**	[N]	7.3	6.8	6.5	6.3	6.1	6.6
	ΔE	[J]	16.8	8.3	8.4	7.0	6.6	9.4
Sample 2	**Max force**	[N]	7.1	6.6	6.3	6.1	6.0	6.4
	ΔE	[J]	16.2	7.7	6.8	7.3	5.7	8.7

Sample 3	**Max force**	[N]	7.9	7.2	6.9	6.6	6.5	7.0
	ΔE	[J]	17.5	8.9	8.0	7.6	6.0	9.6
Sample 4	**Max force**	[N]	7.8	7.1	6.8	6.6	6.4	7.0
	ΔE	[J]	17.2	9.0	6.1	6.0	6.9	9.0
Sample 5	**Max force**	[N]	7.6	7.0	6.7	6.5	6.3	6.8
	ΔE	[J]	16.6	6.8	7.3	5.8	5.3	8.3
Average	**Max force**	[N]	7.6	7.0	6.6	6.4	6.3	6.8
	ΔE	[J]	16.8	8.1	7.3	6.7	6.1	9.0

Table 2

Mean values of energy dissipation and maximum force for varying intestine elongation

3	**7 mm elongation (7%)**						
	stretching						
		1	**2**	**3**	**4**	**5**	**average**
Max force	[N]	4.8	4.5	4.3	4.2	4.1	4.4
ΔE	[J]	10.1	6.0	5.0	4.8	4.4	6.1
	9 mm elongation (10%)						
		1	**2**	**3**	**4**	**5**	**average**
Max force	[N]	7.6	7.0	6.6	6.4	6.3	6.8
ΔE	[J]	16.9	8.1	7.3	6.75	6.1	9.0
	11 mm elongation (13%)						
		1	**2**	**3**	**4**	**5**	**average**
Max force	[N]	10.9	10.0	9.5	9.1	8.9	9.7
ΔE	[J]	28.2	11.5	10.1	9.6	8.8	13.6

Table 3 shows the percentage decrease of maximum forces and energy dissipated for the first and last stretching of the intestine. Figure 7 shows a sample diagram of forces and elongation percentage for the first and fifth longitude elongation.

The next phase of the research focused on intestines' behavior under the greater velocity of stretching and releasing. To do so, the sample was stretched at various velocities. The test started with a stretching (and releasing) velocity of 3.3 mm/s and then it was increased by 8.3 mm/s until it reached a value of 83.3 mm/s.

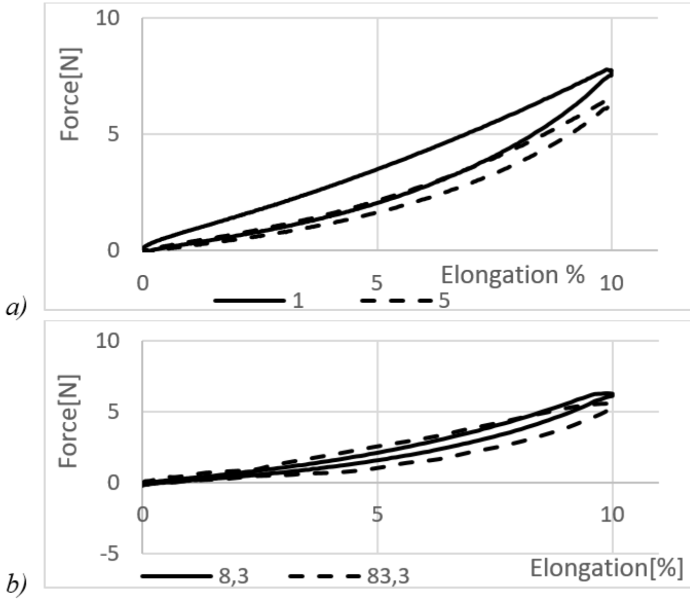

Figure 8
Diagram of intestine elongation by 10%: a) for elongation no. 1 and 5 with 3.3 mm/s velocity; b) with 8.3 mm/s and 83.3 mm/s velocity

Table 3
Mean values of energy dissipation and maximum force for varying intestine elongation

		7 mm elongation (7%)		
		Elongation no.		**Difference**
		1	**5**	**[%]**
Max force	[N]	4.8	4.1	14.6
ΔE	[J]	10.1	4.4	56.4
		9 mm elongation (10%)		
		Elongation no.		**Difference**
		1	**5**	**[%]**
Max force	[N]	7.6	6.3	17.1
ΔE	[J]	16.9	6.1	63.9
		11 mm elongation (13%)		
		Elongation no.		**Difference**
		1	**5**	**[%]**
Max force	[N]	10.9	8.9	18.3
ΔE	[J]	28.2	8.8	68.8

6 Discussion

The obtained results clearly show that the maximum forces of intestinal stretching are greatest during the first stretching and get lower with successive elongations – the lowest values are measured during the fifth elongation. Similar results were obtained for the total energy dissipated in the intestines - the greatest energy value is being lost during the first stretching of each sample and for the longest elongation.

Table 3 and Figure 8a show that for a series of elongations, stretching forces and dissipated energy get smaller. In addition, the results in Table 3 show that for longer elongation, the decrease of dissipation and maximum forces get larger. The presented results indicate that for dynamic interactions, damping properties of the intestines will cause a decrease in the force necessary for another elongation. This can be explained by the decreasing elasticity of samples taken post-mortem, yet this needs to be confirmed during in-vivo experiments.

The next phase of the research focused on intestines' behavior under the greater velocity of stretching and releasing. To do so, the sample was stretched at various velocities. For each velocity, two elongations of the intestines were made and measured values (max force and ΔE) were averaged. Each time between the velocity change there was a break lasting ca. 10 s, the purpose of which was to let the intestines regain their original shape. This interval was selected based on research presented in [14], in which the forces in the intestines stabilized after ca. 10 s (after the elongation). The results of this experiment are presented in Figure 9.

An example diagram for various velocities is presented in Figure 9b. It shows that for increasing velocity, the maximum force drops. The decrease of force in the subsequent repeats of elongations was analogical as in previous tests (Tables 1-3 and Figure 9a).

This phenomenon can be explained by the low ability of samples taken post-mortem to regain their natural shape. This comes with permanent deformation of the samples without causing any actual damage to them. Yet, as a result of energy dissipation increasing with the increase in velocity, it can be stated that these permanent deformations are made at a minimal scale. These are hypothetical theses that need to be confirmed during in-vivo tests. Additionally, the tests show that energy dissipation is greater for faster intestine elongation. This phenomenon can be used to increase the effectiveness of device motion. In summary, the dissipated energy is greater for bigger intestinal elongation and for faster elongation, which is presented in Figure 10.

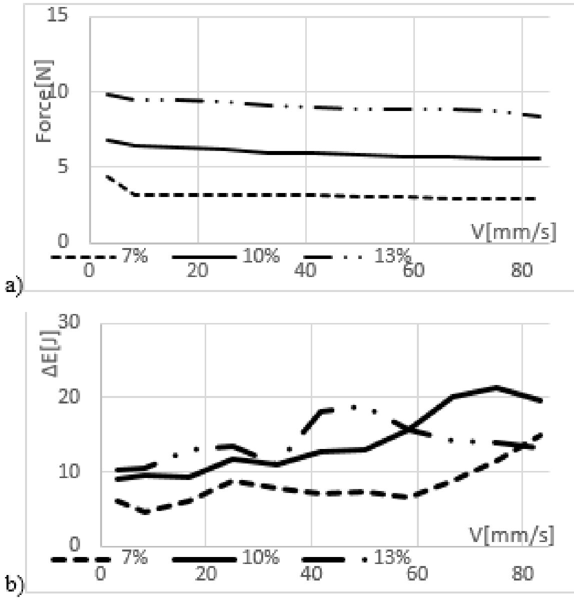

Figure 9
The results of intestine elongation for variety of velocities: a) maximum forces, b) value of dissipated energy

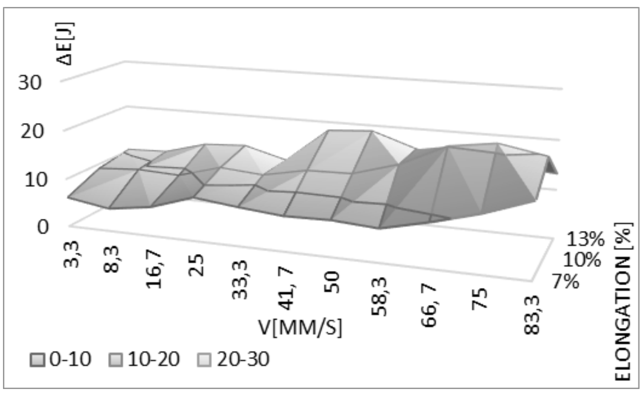

Figure 10
Energy dissipated in the intestines in function of elongation and elongation velocity

Conclusions

The performed experiments show that a series of intestines elongations cause the decrease of forces necessary for subsequent elongations and the decrease of dissipated energy. Tests show that this phenomenon is repeatable, yet it is impossible to state what causes these changes without performing in-vivo tests.

Nevertheless, results show that it is possible to use dissipated energy as the snake-like robot propulsion method.

Another important conclusion is that during the intestine stretching and release, part of the energy is dissipated. Tests show that its value ranges from 4 to 21 J depending on the length and velocity of elongation. It is still necessary to check if the intestines can regain their natural shape during tests with a high velocity between the series. If so, it will result in a lack of energy dissipation. This feature can be used to propel a device that could move inside the intestines using a snake-like motion. The phenomenon of energy dissipation by the intestines during their elongation can hypothetically be a drive for a device moving inside them.

Future works will be focused on creation of the next versions of the robot. It is planned to further increase its length and while decreasing the diameter. Obtained tissues deformation results are to be used as an entry point to perform additional simulations of robot motion inside the intestines. The obtained results of named actions will be the content of future publications.

Acknowledgement

The presented research was co-financed by The National Centre for Research and Development, under LIDER Programme, for 2017-2019, LIDER/20/0106/L-7/15/NCBR/2016

References

[1] Fracczak L, Kobierska A, Koter K, Żak P, Czkwianianc E, Kolejwa M, Nowak A, Socha – Banasiak A, Ślęzak J, The Diagnostic Gastroenterology Needs in Relation to Exisiting Tools, Research and Design Work on a New Tool in Endoscopy Field, Methods and Models in Automation and Robotics (MMAR), 2017 19th International Conference On, pp. 705-710

[2] Fracczak L, Olejniczak M, Podsądkowski L, Long-range snake-like robot powered by pneumatic McKibben muscles, Archive of Mechanical Engineering, Vol. 66, Nr. 2, pp. 257-267, 2019, DOI: 10.24425/ame.2019.128447

[3] L. Fracczak, B. Bryl-Nagórska, P. Żak, A simulation experiment of snake-like robot module, 2018 18th International Conference on Mechatronics - Mechatronika (ME), Brno, 2018, pp. 392-396

[4] Liao D, Frokjaer JB, Yang J, Zhao J, Drewes AM, Gilija OH, Gregersen H. Three-dimensional surface model analysis in the gastrointestinal tract. World J Gastroenterol 2006; 12(18): 2870-2875

[5] Xiaona Wang and M. Q. -. Meng, Study of Frictional Properties of the Small Intestine for Design of Active Capsule Endoscope, The First IEEE/RAS-EMBS International Conference on Biomedical Robotics and Biomechatronics, 2006, BioRob 2006, 2006, pp. 124-129, doi: 10.1109/BIOROB.2006.1639071

[6] Kim JS, Sung IH, Kim YT, Kim DE, Jang YH. Analytical Model Development for the Prediction of the Frictional Resistance of a Capsule Endoscope inside an Intestine. Proc. Inst. Mech. Eng. H. (2007) 221 (8), 837-845

[7] Kim JS, Sung IH, Kim YT, Kwon EY, Kim DE, Jang YH. Experimental investigation of frictional and viscoelastic properties of intestine for microendoscope application. Tribology Letters, Vol. 22, No. 2, May 2006, DOI: 10.1007/s11249-006-9073-0

[8] Zhou H, Alici G, Than TD, Li W. An investigation into biomechanical properties of a real intestine for design of a spiral-type robotic capsule. 2013 IEEE/ASME International Conference on Advanced Intelligent Mechatronics, Wollongong, Australia, July 9-12, 2013

[9] Chen B, Zhou Y, Mu X. Biomechanical behaviour study of dog's small intestines. ISSN 1009-3095 Journal of Zhejiang University SCIENCE V. 3, No. 5, pp. 549-552, Nov.-Dec., 2002

[10] Accoto D, Stefanini C, Phee L, Arena A, Pernorio G, Menciassi A, Carrozza MC, Dario P. Measurements of the frictional properties of the gastrointestinal tract. Scuola Superiore Sant'Anna - MiTech Lab, via Carducci, 40 - 56127 Pisa, Italy

[11] Tan R, Liu H, Su G, Zhang Ch, Li H, Wang Y. Experimental Investigation of the Small Intestine's Viscoelasticity for the Motion of Capsule Robot. Proceedings of the 2011 IEEE, International Conference on Mechatronics and Automation, August 7-10, Beijing, China

[12] Kwon J, Park S, Kim B, Park JO. Bio-Material Property Measurement System for Locomotive Mechanism in Gastro-Intestinal Tract. Proceedings of the 2005 IEEE, International Conference on Robotics and Automation, Barcelona, Spain, April 2005

[13] Zhang Ch, Liu H. Analytical Friction Model of the Capsule Robot in the Small Intestine. Tribol Lett (2016) 64:39, DOI 10.1007/s11249-016-0774-8

[14] Higa M, Luo Y, Okuyama T, Takagi T, Shiraishi Y, Yambe T. Passive mechanical properties of large intestine under in vivo and in vito compresion. Medical Engineering & Physics 29 (2007) 840-844